INTERNATIONAL JOURNAL OF RESEARCHES IN BIOSCIENCES, AGRICULTURE & TECHNOLOGY
© VISHWASHANTI MULTIPURPOSE SOCIETY (Global Peace Multipurpose Society) R. No. MH-659/13(N)
www.vmsindia.org

ELECTROCHEMICAL STUDY OF ELECTROSPUN NANOFIBERS OF PPY/CNT/MNO_2 FOR SUPERCAPACITORS

[1]Mahore R.P., [2]Burghate D.K., [1]Kondawar S.B. and [2]Burghate P.D.

[1]R.T.M. Nagpur University, Nagpur (M.S) India
[2]Shri Shivaji Science College, Nagpur (M.S) India
Email: *ritumahore7@gmail.com*

Abstract: In this paper we report the synthesis and electrochemical study of ternary composites of conducting polymer polypyrrole (PPY) and CNT-MnO_2 so as to use them in device application. Ternary composites of PPY/CNT/MnO_2 have been synthesized by *in-situ* chemical polymerization. Electrospun nanofibers of ternary composite were fabricated by using poly vinylidene fluoride (PVDF) as carrier polymer. Analytical techniques such as SEM, FTIR, and XRD are used to characterize the synthesized ternary composites. The ternary composite showed good interaction based on the shift to longer wavelengths in the electronic transition, indicating the interaction between PPY and CNT-MnO_2 as observed in their FTIR spectra of powder as well as fibers. Crystallinity of MnO_2 in ternary composite was confirmed from XRD results. The SEM images of synthesized ternary composites reveal dispersion of polymer over CNT and the SEM images of fiber indicates the diameter of fibers in the range of 100-300nm. Electrochemical study was done by cylic voltamettry(CV), Galvanostatic Charge-Discharge (GCD) and Electrochemical Impedance Spectroscopy (EIS).

Keywords: Ternary composite, Electrospun nanofibers, Electrochemical study

Introduction:

Today's rapid growth of portable electronic equipment, wireless sensor networks and other micro systems is driving an increasing demand for better energy storage and power supply under various conditions. At the same time, the desire to further miniaturize existing on-chip systems makes it attractive to develop power devices integrated with other elements. Batteries, Fuel cells and Supercapacitors are energy storage devices which are based on the principle of electrochemical energy conversion. In these devices, chemical energy is converted in to electrical energy by means of electrochemical reactions which can be done by electrochemical study [1-4]. According to the charge storage mechanism, Supercapacitors are commonly divided into two main types: electrochemical double layer capacitors (EDLCs) and pseudcapacitors. In general, carbonaceous materials are used as the electrode material of EDLCs which operate on a mechanism involving non-Faradaic reactions taking place between solid state electrode surface and surrounding electrolyte. Whereas, transition-metal oxides as well as conducting polymers are used as the electrode materials of pseudocapacitors in which the capacitance is based on rapid and electrochemically reversible Faradaic redox reactions across the electrode/electrolyte interface [5-8]. Thus, from the view of active material, electrode material for supercapaciotrs can be divided into three categories: carbon materials metal oxides and conductive polymers. The performances of the EDLCs depend strongly on the specific surface area of carbon-based material. Furthermore, its specific capacity is low; the energy density and power density is poor under high current density discharge. On the other hand, pseudocapacitors, typically more than ten times greater than EDLC, its electrode materials mainly including both transition-metal oxides and Conductive polymers such as polypyrrole and polyaniline show high plasticity and easy to form, but its cycle life and thermal stability still need to be improved. However, the poor electrical conductivity of transition metal oxides and instability in high proton conducting mediums greatly diminish the specific capacitance of transition metal oxides, which restricts its application in supercapacitors indicating that pseudocapacitive materials viz. transition metal oxides and conducting polymers have high specific capacitance, but they suffer from low mechanical strength, poor electrical conductivity and low porosity which inhibit their application as supercapacitor electrodes. To overcome the challenges of EDLC's materials and pseudo-capacitive materials, nanostructure containing composites consisting carbon based materials and pseudo-capacitive materials have been synthesized [9-13]. There are mainly four types of nanostructures: zero, one, two and three dimension structures. Among them, one-dimensional (1D) nanostructures have been the focus of quite extensive studies worldwide, partially because of their unique physical and chemical properties. Compared to the other three

dimensions, the first characteristic of 1D nanostructure is its smaller dimension structure and high aspect ratio, which could efficiently transport electrical carriers along one controllable direction, thus are highly suitable for moving charges in intergrated nanoscale systems. The second charateristic of 1D nanostructure is its device function, which can be exploited as device elements in many kinds of nanodevices [14].

1D materials can be used invarious applications where high surface area and porosity are desirable. 1D nanomaterials can be prepared by many methods such as template-directed methods, vapor-phase methods, interface synthesis techniques , solvothermal synthesis, solution-phase growth controlled by capping reagents, nanolithography and self-assembly. However, each of these methods has limitations, such as material restrictions, high cost, and high process complexity. Recently, electrospinning, a simple, inexpensive technique, has attracted significant attention in the preparation of nanomaterials. A typical electrospinning apparatus consists of a syringe, a grounded collector and a high voltage power supply. In a typical fiberspinning process, a syringe is filled with a melt or blend polymer solution and a high voltage (typically kV) is applied between the syringe nozzle and a collector. Electrospinning is fundamentally different from air or other mechanically driven spinning techniques in that the extrusion force is generated by the interaction between the charged polymer fluid and an external applied electric field. During electrospinning, a conical fluid structure called the Taylor cone is formed at the tip of the syringe. At a critical voltage, the repulsive force of the charged polymer overcomes the surface tension of the solution and a charged jet erupts from the tip of the Taylor cone. If the applied voltage is not high enough, the jet will break up into droplets, a phenomenon called Rayleigh instability. If the voltage is sufficiently high, a stable jet will form near the tip of the Taylor cone. Beyond the stable region, the jet is subject to bending instability that results in the polymer being deposited on the grounded collector via a whipping motion. As the charged jet accelerates towards regions of lower potential, the solvent evaporates, and the resulting increase in the electrostatic repulsion of the charged polymer causes the fibers to elongate. The strength of the polymer chains prevents the jet from breaking up resulting in the formation of fibers [15]. In present work, we have made an attempt to synthesize the ternary composite of polypyrrole, CNT and MnO_2(PCM) by in-situ chemical oxidative method and that was fabricated into nanofiber by elelctrospinning (PCM electrospun nanofibers). The electrochemical study was done for the application of supercapacitor.

Experimental:

Synthesis of MnO_2

MnO_2 was synthesized by a refluxing method. Firstly, 4 mmol of $KMnO_4$ powder with a certain amount of $K_2Cr_2O_7$ (molar ratio $K_2Cr_2O_7/KMnO_4$ 0.25:0.1) was dissolved in 150 mL deionized water, and 6 mmol of $MnCl_2$ $4H_2O$ in 150 mL deionized water. The $KMnO_4$ solution was added dropwise into the $MnCl_2$ solution under constant stirring, which resulted in brown precipitation. Then the suspension was heated and refluxed for 2 hrs. After cooling to room temperature naturally, the resulted black solid product was filtered and washed thoroughly with deionized water, and dried at 80°C overnight [16].

Functionalisation Procedure

As-received CNTs were functionalized by chemically treated in the acid solution containing 6M H_2SO_4 and 6M HNO_3 in 3:1 ratio. CNTs were added to the acid solution and then sonicated for 4 hours at 50°C. After centrifugation CNTs were filtered, washed and dried to get functionalized CNTs [17].

Synthesis of PPy/CNT/MnO_2 (PCM) ternary composite

PPy/CNT/MnO_2 nanocomposite was synthesized by an *in-situ* chemical oxidation polymerization. In a typical reaction, 5% of functionalized CNTs (by weight of PPy) and 10% of MnO_2 were first well stirred in 50 mL of an aqueous solution containing 500µL of the pyrrole monomer. This solution was ultrasonicated for 30 min. which facilitated the proper dispersion and interaction of CNTs, MnO_2 and monomer pyrrole. Anhydrous ferric chloride (1.94 g $FeCl_3$) in 50 ml de-ionozed water was slowly added drop wise into this solution and the polymerization was allowed to continue for 4 h with constant stirring. The precipitated composite was filtered, washed thoroughly with de-ionized water, and then dried in a vacuum oven at 60°C for 12 hrs.

Fabrication of PPy/CNT/MnO_2 (PCM) electrospun nanofibers

The ternary composite in powder form was dissolved in NMP and to make the viscous

solution poly vinylidene fluoride (PVDF) was dissolved. Then the solution was vigorously stirred and heated simultaneously for 12 hrs to make a homogenous solution. Electrospun fibers of the ternary composite were produced by electrospinning prepared solution at a potential of 20 kV using a 10 ml syringe with a metal needle, which kept at a distance of 15cm from aluminum collecting drum covered with an aluminum foil. The flow rate was adjusted to be 0.2 ml/hour using a syringe pump. Prepared electrospun fibers were collected on aluminum foil wrapped on rotary drum as collect to obtain well aligned nanofibers

Results and discussion:

FTIR

The FTIR spectrum of PCM shown in Fig.1.(a) shows the characteristic peaks at 3443 cm^{-1} for N-H stretching, 1656 cm^{-1} for C=C stretching, 1467 cm^{-1} and 1396 cm^{-1} for C-C and C-N in-plane stretching, 1211 cm^{-1}, 1064 cm^{-1} for C-H deformation and 810, 722, 579 cm^{-1} for ring torsion. The above bands demonstrate the sample to be PPy chains in the ternary composite with the slight change in the peak values which may be attributed due to presence of CNTs. Further, the peak at 722 cm^{-1} can be assigned to Mn-O stretching vibrations indicating the existence of MnO_2 in the ternary composite. Fig.1.(b) shows the FTIR spectra of PCM electrospun nanofibers which shows the slight shift in the peaks values with the characteristics peaks of PVDF 800 cm^{-1}[18].

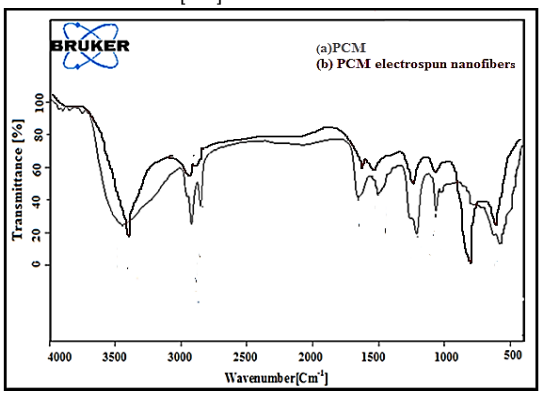

Fig.-1. FTIR spectra of (a) PCM and (b) PCM electrospun Nanofibers.

SEM

The morphology of ternary nanocomposite PCM is depicted in Fig.2. (a). The image shows the existence of tubular interwoven, mixed rough and granular morphology which are characteristic morphologies of CNTs, MnO_2 and Polypyrrole. Here the MnO_2 particles are believed to present not only on the surface of the composite but also in the interior of the composite three dimensionally. CNTs are hardly observable from these images. This indicates that the CNTs are well-coated with the Polypyrrole and MnO_2. The continuous well aligned nanofibers of ternary composite with the diameter in the range of 250 – 430 nm as shown in Fig. 2.(b). The present composite material appears to have uniform distribution of these three individual components and it also bears pores on the surface. One dimensional ternary composite materials are useful in supercapacitor due to their large aspect ratio and porosity apart from high surface to volume ratio [19].

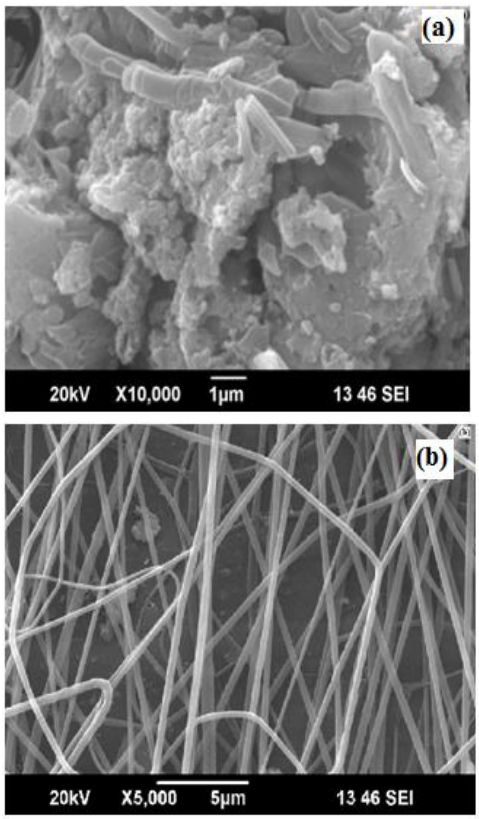

Fig.-2. SEM images of (a) PCM and (b) PCM electrospun nanofibers

XRD

Fig.3. shows the XRD patterns of (a) PCM and (b) PCM electrospun nanofibers. XRD pattern exhibits a broad characteristic peak at 2θ = 25° broad characteristic peak at about 25° of pure PPy exhibits that pure PPy is amorphous, implying an amorphous structure [20,21]. The diffraction peaks at 2θ= 28.81°, 37.41°, 49.81° and 60.21° can be indexed to a pure tetragonal phase of α-MnO2 (JCPDS 44-0141). Good crystallinity is evidenced by the strong diffraction peaks are observed. No other characteristic impurity peaks are observed, indicating the high purity of α-MnO_2 [22, 23]. Sharp and high intensity peak at 25.9°and a lower intensity peak at 44.4° which attributes to the diffraction signature of the distance between the walls of CNT and the internal spacing. PCM shows the diffraction peaks of every individual material. In Fig.3.(b) XRD pattern of PCM electrospun nanofibers all the characteristics peaks of individual material can be seen with broad and intense peak is seen which is due the presence of PVDF which was added to form the electrospun nanofiber.

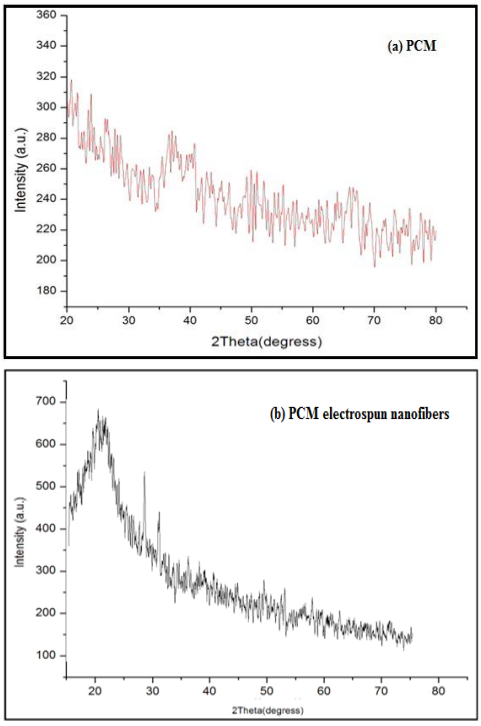

Fig.-3. XRD patterns of(a) PCM and (b) PCM electrospun nanofibers.

Electrochemical performances

The electrochemical characterization of the ternary composites was performed using an electrochemical workstation in Na_2SO_4 (1M) solution. Ag/AgCl reference electrode and Pt counter electrode were used in the measurement. Cyclic voltammetry (CV) was carried out at different scan rates with a potential window from -0.1 to 0.9 V. Galvanostatic charge/discharge tests were measured at a specific current of 2A g^{-1}. The electrochemical impedance spectroscopy (EIS) measurements were conducted in the frequency from 100 kHz to 20 mHz with perturbation amplitude of 5 mV versus the open circuit potential.

Cyclic voltammograms(CV) of PPy/CNT/ MnO_2

Fig.4. (a) and (b) exhibits CV at scan 50mV/s and 100mV/s scan rate respectively. CV curve is relatively rectangular in shape and exhibits a mirror-like replication. No visible redox peaks were observed, implying the stability of the electrolyte. The shape of the CV curves is symmetric in both the scan rates. This suggests high efficiency of the capacitive characteristics at the electrode/electrolyte interface. The area under CV curve divided by scan rate gives the value of capacitance. The shape of the CV curves is symmetric in both the scan rates which can beneficial for reversibility of electrode. This suggests high efficiency of the capacitive characteristics at the electrode/electrolyte interface [24].

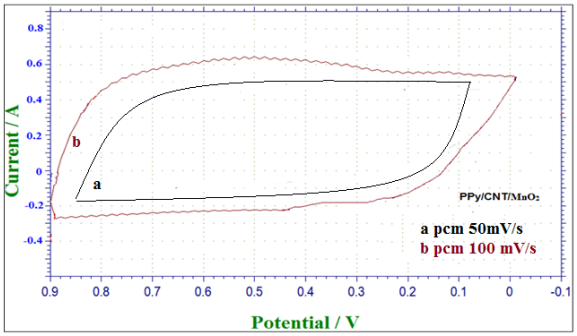

Fig.-4. Cyclic voltammogram for PPy/CNT/ MnO_2

Cyclic voltammograms of PPy/CNT/MnO_2 electrospun nanofibers

Fig.5. illustrates cyclic voltammograms of PPy/CNT/MnO_2 (PCM) electrospun nanofiber at various scan rates. Cyclic

voltammetric scanning was performed in an aqueous solution of 1M Na_2SO_4 with a potential window -1.0 to +0.8V versus Ag /AgCl. In Fig.5.(a) and (b) exhibits CV at scan 50mV/s and 100mV/s scan rate respectively. CV curve is relatively rectangular in shape and exhibits a mirror-like replication which revealed an excellent rate capacitance performance. The distort from rectangular shape of CV curves with increase of scan rate was ascribed to polarization intensity which increased with increase of scan rate and kinetically limited the electrolyte ions from penetrating into active materials [25]. During the reaction of pyrrole, concurrent growth of MnO_2 with PPy generates uniform and ordered structures that lead to efficient performance in charge storage. Furthermore, the improved electronic conduction by the molecular level interactions of MnO_2, CNT and PPy results in high rate capability in electrochemical electrode. During the redox cycling, mass insertion/ejection takes place in the polymer chains, and the repetitive swelling/shrinkage causes chain defects in the polymer matrix, deteriorating the mechanical stability and electronic conduction of the electrode. The deterioration in CV performance at high scan rates in Fig.5 (b) supports the inference that the molecular level dispersion of MnO_2 in PPy matrix has an important effect on PPy/CNT/MnO_2 conductivity [26].

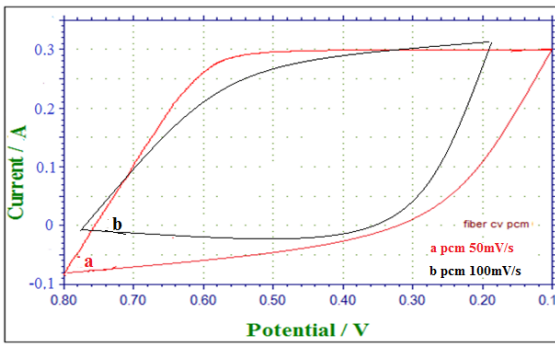

Fig.-5. Cyclic voltammograms of PPy/CNT/ MnO_2 electrospun nanofibers

Galvanostatic Charge-Discharge curves of PCM and PCM electrospun nanofibers

Capacitance behaviours and cyclic life of PPy/CNT/MnO_2 and PPy/CNT/MnO_2 electrospun nanofibers coatings on stainless steel electrodes were studied by chronopotentiometry , by subjecting them to galvanostatic charge–discharge cycling. The specific capacitance of electrodes was calculated from the discharge curves using the following equation:

$$C_s = \frac{I\,\Delta t}{m\,\Delta V}$$

Where C_S (F g^{-1}) is the specific mass capacitance, I is the current (A), and Δt is the discharge time (s), ΔV is the potential window and m is the total mass of active material (g) [27]. The specific capacitance of PCM electrospun nanofibers was calculated 427 F/g and PCM is 405F/g.

Fig.6. (a) and (b) the Galvanostatic Charge-Discharge curves of PPy/CNT/MnO_2 (PCM) and PPy/CNT/MnO_2 (PCM) electrospun nanofibers respectively at the current density of 2A/g. Charge–discharge experiments were performed from -0.05 to 0.45 V. The GCD curves have approximately equal charging and discharging times, implying a favourable electrochemical reversibility. The charge-discharge curves were symmetrical and indicated good electrochemical efficiency. The IR drops of the PPy/CNT/MnO_2 (PCM) electrospun nanofibers are lower than that and PPy /CNT/ MnO_2 (PCM) composites, reflecting the higher internal resistance for PCM in contrast to the PPy/CNT/MnO_2 (PCM) electrospun nanofibers. Due to this lower internal resistance, less energy will be wasted to produce unwanted heat during charge/discharge
process in energy storage devices. Thus, the PPy/CNT/MnO_2 (PCM) electrospun nanofibers can be better material for device application. It also can be seen that the charge/discharge duration of the PPy/CNT/MnO_2 electrospun nanofibers composite is larger than that of PCM, confirming the highest specific capacitance for the PPy/CNT/MnO_2 electrospun nanofibers composite electrode [28, 29].

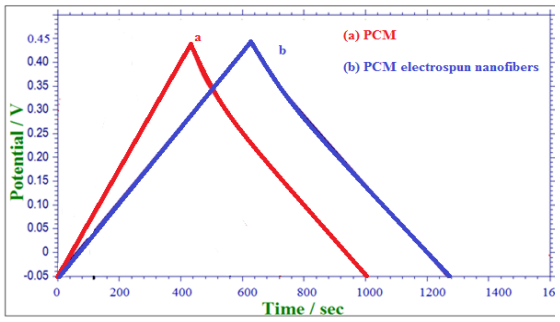

Fig.-6. GCD of (a)PCM and (b)PCM eletcrospun Nanofibers

EIS for PCM composites and PCM electrospun nanofibers

In Nyquist plot, the real axis intercept represents the equivalent series resistance (ESR), including the contact resistance and the intrinsic resistance of the active materials and the electrolyte, smaller ESR values imply the higher conductivity, smaller diameter of the semicircle in represents the lower charge transfer resistance and the vertical line in a low frequency range indicates the nearly ideal capacitive behaviors. The same resemblance can be seen in Nyquist plot Fig.6.(a) PPy/CNT/MnO_2 (PCM) and (b) PPy/CNT/MnO_2 (PCM) electrospun nanofibers. The values of Rs, Rp and ESR for all the materials determined from the data in Fig.6.(a) and (b) are listed in Table1.

Table-1. Rs, Rp and ESR values of PCM and PCM electrospun nanofibers.

Material	Rs (Ω)	Rp (Ω)	ESR
PCM	0.2	2.75	2.55
PCM electrospun nanofiber	0.1	1.80	1.7

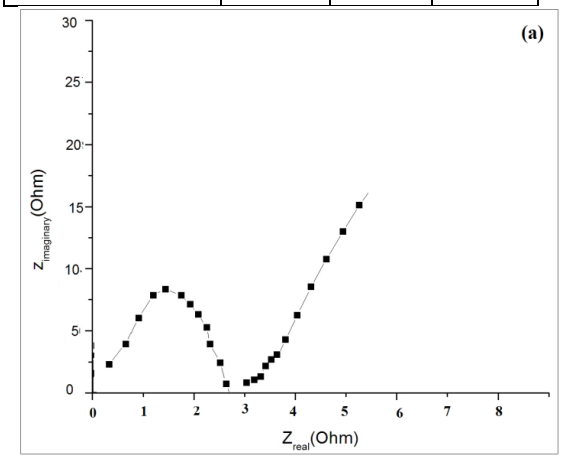

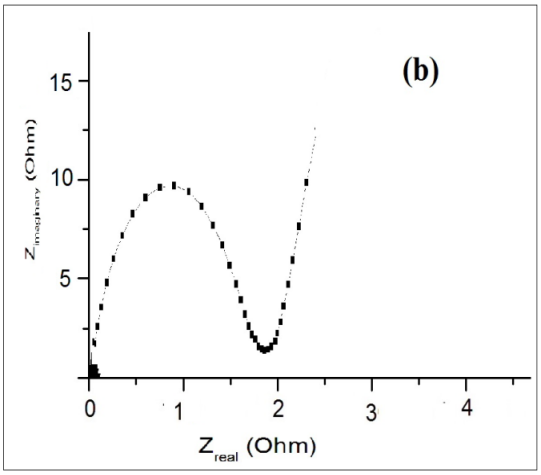

Fig.7.Nyquist plot for (a) PCM (b) PCM electrospun nanofibers

Conclusions:

Polypyrrole/CNT/MnO_2 (PCM) have been synthesized by in-situ chemical oxidative method. Polypyrrole/CNT/MnO_2 (PCM) eletcrospun nanofibers were perepared by electrospinning by preparing a viscous solution with NMP and PVDF. The as prepared materials were characterized by Scanning electron microscopy (SEM), Fourier Transform Infrared Spectroscopy (FT-IR) and X-Ray diffraction (XRD). The FTIR spectra of PCM shows all the characteristics of individual components and the FTIR of PCM electrospun nanofibers which shows the slight shift in the peaks values with the characteristics peaks of PVDF 800 cm^{-1} The SEM images show the existence of tubular interwoven, mixed rough and granular morphology which are characteristic morphologies of CNTs, MnO_2 and Polypyrrole. Here the MnO_2 particles are believed to present not only on the surface of the composite but also in the interior of the composite three dimensionally. CNTs are hardly observable from these images. This indicates that the CNTs are well-coated with the Polypyrrole and MnO_2. The continuous well aligned nanofibers of ternary composite with the diameter in the range of 250 – 430 nm. The XRD pattern of PPy/CNT/MnO_2 the diffraction peaks of every individual material is clearly seen. The electrochemical analytical techniques viz. Cyclic Voltamettry (CV), Galvanostatic Charge –Discharge

(GCD) and Electrochemical Impedance Spectroscopy (EIS) was carried out in a three electrode compartment cell of all the materials under investigation. Ag/AgCl was used as the reference electrode, and a platinum wire was employed as the counter electrode. The electrochemical study of PCM electrospun nanofibers is found to be better than the PCM nanocomposite.

Acknowledgement

The present work was supported by University Grant Commission (UGC), New Delhi, India under Major Research Project No 41-931/2012. The authors are thankful to UGC for financial support to carry out this work.

References:

K. Karthikeyan, D. Kalpana, N. G. Renganathan, Ionics, 15, 2009, 107-110

S.Chen, R.Ramachandran, V.Mani, R.Saraswathi. International journal of Electrochemical Science, 9, 2014, 4073

C.Shen, X.Wang, W.Zhanga, F.Kang, Journal of Power Sources 196 ,2011,10465–1047

X.Mao, T. A.Hatton, Gregory C. Rutledge COC 17, 2013,1390–1401

Y. Zhang, H. Feng, X. Wu, L. Wang, A. Zhang, T. Xia, H. Dong, X. Li, L. Zhang, , Int. J. Hydrog. Energy 34 , 2009, 4889.

C.D. Lokhande, D.P. Dubal, O.-S. Joo, Metal oxide thin film based supercapacitors, Curr. Appl. Phys. 11 ,2011, 255.

A. Wang, H. Wang, S. Zhang, C. Mao, J. Song, H. Niu, B. Jin, Y. Tian, Controlled synthesis of nickel sulfide/graphene oxide nanocomposite for highperformance supercapacitor, Appl. Surf. Sci. 282 , 2013,704.

R. Kötz, M. Carlen, Principles and applications of electrochemical capacitors, Electrochim. Acta 45 ,2000, 2483.

Raj Kishore Sharma, Lei Zhai. Electrochimica Acta 54 (2009) 7148–7155

Yanfang Yan, Qilin Cheng, Vladimir Pavlinek, Petr Saha, Chunzhong Li. Electrochimica Acta 71 (2012) 27– 32

Wenjuan Wang, Wu Lei, Tianyuan Yao, Xifeng Xia, Wenjing Huang, Qingli Hao, Xin Wang. Electrochimica Acta 108 (2013) 118– 126

Yuhong Jin, Mengqiu Jia. Colloids and Surfaces A: Physicochem. Eng. Aspects 464 (2015) 17–25

Yong Zhang, Guang-yin Li , Yan Lv , Li-zhen Wang, Ai-qin Zhang ,Yan-hua Song , Bei-li Huang. international journal of hydrogen energy 36, 2011,11760-11766

R. Mahore, D. Burghate, P. Burghate, S. Kondawar, P. Patil, B. Meshram, International Journal of Biosciences, Agriculture and technology,1,2014,2347-517x

Zexuan Dong, Scott J. Kennedy, Yiquan Wu, Journal of Power Sources 196 (2011) 4886–4904

L. Chen, Z. Song, G. Liu, J. Qiu, C. Yu, J. Qin, L. Ma, F. Tian, W. Liu. Journal of Physics and Chemistry of Solids, 74, 2013, 360–365.

R. Mahore, D. Burghate, S.Kondawar, Advance Material Letter, 7, 2014,400-405

Saiful Izwan Abd Razak, Abdul Latif Ahmad and Sharif Hussein Sharif Zein, (2009). *Journal of Physical Science,* 20 27–34

R.Mahore, S. Kondawar, D. Burghate, B. Meshram, Journal of the Chinese Advanced Materials Society,3,2014, 45-56.

B. Wang, J. Qiu, H. Feng, E. Sakai, Electrochimica Acta, 151, 2015, 230–239.

N. Su, H. Li, S. Yuan, S. Yi, E. Yin, EXPRESS Polymer Letters, 6, 2012, 697–705.

L. Chen, Z. Song, G.Liu, J.Qiu, C.Yu, J. Qin, L.Ma, F. Tian, W. Liu, Journal of Physics and Chemistry of Solids, 74, 2013, 360–365.

W. Yao, H.Zhou, Y. Lu, Journal of Power Sources, 241,2013, 359-366.

T. Zheng, X. Lu, X. Bian, C. Zhang, Y. Xue, X. Jia, C. Wang, Talanta, 90, 2012, 51– 56.

S. He, L. Chen, C. Xie, H. Hu, S. Chen, M. Hanif, H. Hou, Journal of Power Sources, 243, 2013, 880-886.

R. K. Sharma, A. Karakoti, S. Seal, L. Zhai, Journal of Power Sources, 195, 2010, 1256–1262.

Y. Zhu, K. Shi, I. Zhitomirsky, Journal of Power Sources, 268, 2014, 233-239.

M. Ramezani, M. Fathi, F. Mahboubi, Electrochimica Acta, 174, 2015, 345–355.

B. Yin, S. Zhang, Y. Jiao, Y. Liu, F. Qu, X. Wu, Cryst Eng Comm, 16, 2014, 9999.

****